Published in final edited form as:
Chromosoma. 2014 March ; 123(0): 147–164. doi:10.1007/s00412-013-0438-5.

Dynamics of DOT1L localization and H3K79 methylation during meiotic prophase I in mouse spermatocytes

David Ontoso[1], **Liisa Kauppi**[2,3], **Scott Keeney**[2], and **Pedro A. San-Segundo**[1,*]

[1]Instituto de Biología Funcional y Genómica. Consejo Superior de Investigaciones Científicas/ University of Salamanca. 37007 Salamanca. Spain

[2]Molecular Biology Program, Memorial Sloan-Kettering Cancer Center, 1275 York Avenue, New York, NY 10065, USA

Abstract

During meiotic prophase I, interactions between maternal and paternal chromosomes, under checkpoint surveillance, establish connections between homologs that promote their accurate distribution to meiotic progeny. In human, faulty meiosis causes aneuploidy resulting in miscarriages and genetic diseases. Meiotic processes occur in the context of chromatin, therefore histone post-translational modifications are expected to play important roles. Here, we report the cytological distribution of the evolutionarily conserved DOT1L methyltransferase and the different H3K79 methylation states resulting from its activity (mono-, di- and tri-methylation; H3K79me1, me2 and me3, respectively) during meiotic prophase I in mouse spermatocytes. In the wild type, whereas low amounts of H3K79me1 are rather uniformly present throughout prophase I, levels of DOT1L, H3K79me2 and H3K79me3 exhibit a notable increase from pachynema onwards, but with differential subnuclear distribution patterns. The heterochromatic centromeric regions and the sex body are enriched for H3K79me3. In contrast, H3K79me2 is present all over the chromatin, but is largely excluded from the sex body despite the accumulation of DOT1L. In meiosis-defective mouse mutants, the increase of DOT1L and H3K79me is blocked at the same stage where meiosis is arrested. H3K79me patterns, combined with the cytological analysis of the H3.3, γH2AX, macroH2A and H2A.Z histone variants, are consistent with a differential role for these epigenetic marks in male mouse meiotic prophase I. We propose that H3K79me2 is related to transcriptional reactivation on autosomes during pachynema, whereas H3K79me3 may contribute to the maintenance of repressive chromatin at centromeric regions and the sex body.

Keywords

Meiosis; DOT1L; H3K79; histone modification; spermatogenesis

Introduction

Meiosis is a specialized cell division that generates haploid gametes required for sexual reproduction because two rounds of chromosome segregation are preceded by a single phase of DNA replication. In order to accomplish this reduction in the number of chromosomes, a sequence of finely regulated, coordinated and monitored events takes place. Thus, the unique meiotic prophase I is the most prolonged and elaborate stage of meiosis, during which pairing, synapsis and recombination between homologous chromosomes occur

*Corresponding author: pedross@usal.es, Phone: (34) 923294902, FAX: (34) 923224876.
[3]present address: Research Programs Unit (Genome-Scale Biology) and Institute of Biomedicine (Biochemistry and Developmental Biology), University of Helsinki, Haartmaninkatu 8, Helsinki, FIN-00014, Finland

(Cohen et al. 2006). Meiotic recombination begins with programmed D N A double-strand breaks (DSBs), introduced by Spo11 and accessory proteins (Keeney 2008). In many organisms, including budding yeast and mouse, meiotic DSBs trigger a complex program in which their repair is coupled to homologous chromosome pairing and synapsis. Interactions between homologs are stabilized by a proteinaceous structure, the synaptonemal complex (SC), which keeps homologs tightly associated during pachynema and facilitates completion of crossover recombination to generate physical linkages required for the subsequent accurate segregation (Pawlowski and Cande 2005). Progression and completion of meiotic events are monitored by checkpoints, specific surveillance mechanisms that block meiotic progression in response to defects and, in the case of Metazoa, lead to apoptosis of aberrant meiocytes avoiding generation of aneuploid gametes (Hochwagen and Amon 2006; Macqueen and Hochwagen 2011)

Meiotic recombination takes place in the context of chromatin; accordingly, several histone post-translational modifications (PTMs) have been found to influence various aspects of meiosis (Bolcun-Filas and Schimenti 2012; Brachet et al. 2012). For example, there is an association between trimethylation of histone H3 at Lysine 4 (H3K4me3) and the determination of meiotic DSB sites, mediated by the Set1 complex and its subunit Spp1 in yeast (Borde et al. 2009; Acquaviva et al. 2013; Sommermeyer et al. 2013) and the meiosis-specific histone H3 methyltransferase PRDM9 in mouse (Baudat et al. 2010; Grey et al. 2011; Smagulova et al. 2011).

Another histone PTM with a known meiotic function is the methylation of H3K79 mediated by Dot1 in *Saccharomyces cerevisiae*. In yeast, H3K79me is largely dispensable for unperturbed meiosis, but it is essential for meiotic recombination checkpoint function (San-Segundo and Roeder 2000; Ontoso et al. 2013). Dot1 is the only methyltransferase responsible for catalyzing mono-, di- and trimethylation at H3K79 in a non-processive manner (Lacoste et al. 2002; van Leeuwen et al. 2002; Ng et al. 2002; Frederiks et al. 2008). To date, there is no demethylase known capable of reverting H3K79me. With a few exceptions, such as for example *Schizosaccharomyces pombe*, which lacks Dot1 and H3K79me, this histone methyltransferase has been conserved through evolution; the mammalian homolog is called DOT1L (for Dot1-like) (Feng et al. 2002; Jones et al. 2008). In human cells and *Drosophila*, DOT1L/dDot1 has been isolated forming part of a large macromolecular complex, DotCom, which modulates its activity (Mohan et al. 2010). DOT1L-mediated H3K79me performs important roles in transcriptional regulation (Steger et al. 2008; Kim et al. 2012a) and affects multiple biological processes (Nguyen and Zhang 2011). In particular, DOT1L activity is involved in embryonic development and differentiation (Jones et al. 2008; Barry et al. 2009), cardiac function (Nguyen et al. 2011), hematopoiesis (Feng et al. 2010; Jo et al. 2011), cell proliferation and aging (Kim et al. 2012b) and chondrogenesis (Castaño Betancourt et al. 2012). Alteration of DOT1L function is related with some types of mixed lineage leukemia (Okada et al. 2005; Krivtsov et al. 2008; Bernt et al. 2011), neural tube defects (Zhang et al. 2013) and osteoarthritis (Castaño Betancourt et al. 2012). The discovery of an increasing number of pathologies related with altered DOT1L-mediated H3K79me patterns points to DOT1L as a promising therapeutic target (Daigle et al. 2011; Yao et al. 2011; Anglin et al. 2012). However, little is known about DOT1L activity in mammalian meiosis; only a study on H3K79me2/3 in mouse oocytes and preimplantation embryos has been reported (Ooga et al. 2008).

Here, we report the characterization of DOT1L localization and the chromatin distribution of the distinct H3K79 methylation states (me1, me2 and me3) during meiotic prophase I in spermatocytes of wild-type mice and various meiotic mutants. Our results reveal a progressive increment of DOT1L activity as prophase I advances, and the existence of differential spatio-temporal patterns for H3K79me2 and H3K79me3. Furthermore, the

comparison of the distribution of these epigenetic marks with that of the H3.3, γH2AX, macroH2A and H2A.Z histone variants hints at a functional contribution of H3K79me2 and H3K79me3 to the characteristic transcriptional states of the different subnuclear territories in spermatocyte nuclei.

Materials and methods

Mice

Animals in this study were of C57BL/6 background or C57BL/6 X 129/Sv mixed background. The *Spo11β*-only transgenic mice, the hypomorphic *Trip13*$^{mod/mod}$, and the *Spo11*$^{-/-}$ and *Dmc1*$^{-/-}$ null mice were previously described (Pittman et al. 1998; Baudat et al. 2000; Roig et al. 2010; Kauppi et al. 2011). To minimize variability due to strain background in the studies involving mutant mice, experimental animals were compared to control animals from the same litter. Experiments conformed to relevant regulatory standards and were approved by the MSKCC Institutional Animal Care and Use Committee.

Immunofluorescence

Mouse testicular cells were prepared for surface spreading and subsequent immunofluorescence as previously described (Barchi et al. 2005), with slight modifications. Testis cell preparations were resuspended in 0.1 M sucrose were added onto glass slides previously coated with a 1% paraformaldehyde, 0.1% Triton X-100 solution, incubated for 3 hours in a humidified chamber at room temperature, rinsed in 0.4% Kodak Photo-Flo 200 and dried briefly. Slides were treated with blocking/antibody dilution buffer (B/ADB: 2 mg/mL BSA, 0.05% Tween-20, 0.2% gelatin in PBS) for 30 minutes at room temperature, and incubated overnight at 4°C with the primary antibody diluted in B/ADB. After four washes of 5 minutes with B/ADB, slides were incubated with the secondary antibody diluted in B/ADB for 1 h at 37°C in the dark. After four washing steps again, slides were mounted in Vectashield mounting medium (Vector) with 5 μg/mL DAPI. Images were captured using an Axio2 microscope (Zeiss) connected to a CCD camera and processed using the SlideBook software package (Intelligent Imaging Innovations).

The following primary antibodies and dilutions were used. Rabbit polyclonal anti- DOT1L (ab64077; 1:200 dilution), anti-H3K79-me1 (ab2886; 1:1000 dilution), anti-H3K79-me2 (ab3594; 1:2000), anti-H3K79-me3 (ab2621; 1:2000 dilution), anti-histone H3 (ab1791; 1:100), and anti-histone H3.3 (ab62642; 1:400) were from Abcam. Mouse monoclonal anti-γH2AX (05-636; 1:800), rabbit polyclonal anti-H2A.Z (07-594; 1:400) and rabbit polyclonal anti-macroH2A (07-219; 1:400) were from Millipore. Mouse monoclonal anti-SYCP3 (sc-74569; 1:500) was from Santa Cruz and goat polyclonal anti-SYCP3 (1:400) was from Terry Ashley.

The following secondary antibodies conjugated with Alexa Fluor were from Molecular Probes and used at 1:200 dilution. Anti-rabbit-AF488 (A-21206), anti-mouseAF594 (A-21203), anti-mouse-AF647 (A-31571), and anti-goat-AF594 (A-11058).

Quantification of fluorescence intensities of individual nuclei was performed with the ImageJ 1.47f software (National Institutes of Health, USA; http://imagej.nih.gov/ij/). The contours of the nuclei, the centromeric areas and the sex bodies were identified based on DAPI and SYCP3 staining. The intensity values within these regions of interest were quantified. Background signal was subtracted using the Otsu's entropy threshold methods in ImageJ. This threshold tool was also used to reproducibly outline without bias the more intense DAPI-stained centromeric regions and the sex body, as shown in Fig. 2. The parameters used for quantification purposes were the integrated density (the result of

multiplying the area by the mean of the fluorescence intensity values) and the percentage of area with signal from the total area of interest.

For graphs showing centromeric regions/uncondensed chromatin ratios (Fig. 2e and Supplementary Fig. 4b, d), a threshold was fixed in every image; then, the percentage of area with DOT1L or H3K79me signal was obtained for all the centromeric regions and a mean value was calculated (numerator). The signal was also measured for the uncondensed chromatin (the whole nucleus except the centromeric regions and the sex body) (denominator). Finally, a ratio between these two values was calculated for each nucleus. The graphs show the mean of these ratios.

For graphs showing XY body/whole nucleus ratios (Fig. 2f and Supplementary Fig. 4a, c) a threshold was fixed in every image. The percentage of area with DOT1L or H3K79me signal was obtained for the XY body (numerator), and for the remaining of nucleus (denominator). A ratio between these two values was calculated for each nucleus. The graphs show the mean of these ratios.

For pairwise comparisons of mutants versus controls, two-tailed Mann–Whitney tests were applied and *P*-values were calculated using the GraphPad Prism 5.0 software (http://www.graphpad.com/)

Bioinformatics

The protein sequence alignment was performed with CLUSTALW (http://www.ebi.ac.uk/Tools/msa/clustalw2/). The PDB ID references for human nucleosomes containing histone variant H3.1, H3.2 and H3.3 are 3AFA, 3av1 and 3av2, respectively (Tachiwana et al. 2010; Tachiwana et al. 2011), available at the Research Collaboratory for Structural Bioinformatics (RCSB) Protein Data Bank (http://www.rcsb.org/pdb/). Molecular graphics and H3K79 highlighting were performed with the UCSF Chimera package (http://www.cgl.ucsf.edu/chimera)

Results

Spatial and temporal patterns of DOT1L and H3K79me distribution during meiotic prophase I

To investigate the localization of mammalian DOT1L and the associated mono-, di- and tri-methylation of histone H3 at lysine 79 (H3K79me1, me2, and me3, respectively) we performed immunofluorescence of surface-spread meiotic chromosomes from wild-type mouse spermatocytes. We tracked SYCP3, a component of the axial/lateral elements of the SC (Lammers et al. 1994), to define the stage of prophase I of each spermatocyte nucleus based on the degree of synapsis exhibited by the chromosomes (Fig. 1 and Supplementary Fig. 1). At the beginning of prophase I, short stretches of SYCP3 start to develop during leptonema. At zygonema, synapsis of homologs begins and thickened SYCP3 areas along the already synapsed regions are detected. At pachynema, synapsis between the autosomes is completed, resulting in a thick and uniform SYCP3 signal. A subnuclear domain formed by the sex chromosomes, the so-called “XY body” or “sex body”, begins to emerge around the end of zygonema, and is fully formed in pachynema. This chromosome pair displays a short synapsed area on a limited distal region of homology, the pseudoautosomal region (PAR). The PAR exhibits thickened SYCP3 staining, whereas a thinner signal is visible along the unsynapsed non-homologous regions (for example, see yellow arrows in Fig. 1a and Supplementary Fig. 1, where the sex body is pointed). At diplonema, homologs progressively desynapse revealing spaces between the SYCP3 axes, but they still remain joined at chiasmata sites where crossovers have occurred. In addition, from late pachynema,

but more evident during diplonema, the chromosomes show thickenings at the ends, which correspond with their attachment to the inner nuclear membrane (Liebe et al. 2004). Meanwhile, in the sex body desynapsis also occurs, the X and Y chromosomes are joined end-to-end, and the X chromosome shows thickenings along its length (Supplementary Fig. 1, diplotene panels). At diakinesis-metaphase I, SC disassembly is general, SYCP3 staining is mainly concentrated at the centromeric areas, and only remnants persist on chromosome arms. The X chromosome remnants are the last ones to disappear (Supplementary Fig. 1, diaki.-meta. panels) (Barchi et al. 2008; Parra et al. 2004)

First, we monitored DOT1L localization throughout meiotic prophase I (Fig. 1a). Interestingly, we found a progressive increment of the association of this histone methyltransferase with meiotic chromatin correlating with the progression through prophase I stages. DOT1L nuclear staining started at very low levels at leptonema, increased slightly in zygonema, followed by a dramatic increment in DOT1L levels at pachynema and, especially, during the diplonema and diakinesis stages (Fig. 1a). The sex body exhibited particularly dynamic patterns, detailed below.

Next, we analyzed the distribution of the three possible methylated states of H3K79 resulting from DOT1L action: H3K79me1, -me2 and –me3 (Fig. 1b–d, respectively). Overall levels of H3K79me1 were uniformly weak at all stages (Fig. 1b). In contrast, H3K79me2 exhibited a progressive enrichment concurrent with prophase I progression, achieving relatively strong staining during pachynema, diplonema and diakinesis/metaphase I (Fig. 1c). H3K79me3 staining also intensified during meiotic prophase I, reaching the highest levels in diakinesis/metaphase I (Fig. 1d).

These observations indicate that overall levels of chromatin-associated DOT1L and H3K79 methylation undergo significant change during male mouse meiotic prophase I. The enrichment of DOT1L is accompanied by higher amounts of two particular methylation states, H3K79me2 and H3K79me3; however, their dynamics and subnuclear distribution were different.

We examined DOT1L and H3K79me in more detail starting from the stage when they became more abundant, pachynema, and focused on the distinctive chromatin regions that can be distinguished according with their intensity of DAPI staining and chromosome positioning, marked by SYCP3. In this way, we discriminated areas with weaker DAPI fluorescence signal, corresponding to euchromatin and encompassing most of the autosome domains. On the other hand, subnuclear territories with more intense DAPI staining were classified into two groups: the constitutive heterochromatin located at the centromeric regions surrounding one end of each mouse autosome (which are telocentric; Kalitsis et al. 2006), and the facultative heterochromatin of the sex body (differentially outlined in Fig. 2a–d). We quantified the signal intensity of DOT1L and the different H3K79me states in the DAPI-bright regions relative to the remaining chromatin (Fig. 2e). Strikingly, we found that, as soon as the large centromeric regions became apparent after mid-zygonema, they exhibited strong accumulation (about 7-fold) of H3K79me3 (Fig. 2d, e). These areas continued to be highly trimethylated at H3K79 through metaphase I, enclosing the centromere-proximal SYCP3 remnants (Parra et al. 2004). Furthermore, strong H3K79me3 staining could be still detected at the chromocenter in round spermatids (Fig. 3). In contrast, neither DOT1L, H3K79me1, nor H3K79me2 showed this centromeric accumulation (Fig. 2a–c), with ratios relative to euchromatin regions close to 1 (Fig. 2e), denoting a more uniform distribution between both types of subnuclear territories.

Sex body development involves massive chromatin remodeling events to establish a heterochromatin configuration that leads to a transcriptional inactivation program, the so-

called “meiotic sex chromosome inactivation” (MSCI) (Handel 2004; Turner 2007). Little is known about the contribution of DOT1L and H3K79me to MSCI, so we analyzed their distribution in the sex body from pachynema to metaphase I (Fig. 2a–d, f). At pachynema, the amount of DOT1L in the sex body was roughly at the average level of the rest of the nucleus, but during diplonema and at diakinesis-metaphase I it significantly increased (two- and four-fold, respectively) (Fig. 2a, f). H3K79me1 maintained a stable, relatively uniform pattern over the entire nucleus at all stages (Fig. 2b, f), while H3K79me2 was under-represented in the sex body from pachynema up to diakinesis/metaphase I (Fig. 2c, f). Finally, XY-associated H3K79me3 started at low amounts during pachynema, matched autosome levels at diplonema and reached a two-fold higher level at diakinesis-metaphase (Fig. 2d, f). In more advanced stages of spermatogenesis, such as in round spermatids, the more intense DAPI-stained territory adjacent to the chromocenter contains the sex chromosome X or Y (Greaves et al., 2006). We found that H3K79me3 was also detected in this region, although at lower levels than in the chromocenter (Fig. 3).

Thus, DOT1L and the ensuing H3K79me states exhibit characteristic spatio-temporal dynamics suggestive of possible differential roles during male mouse meiotic prophase I.

Impaired DOT1L localization and H3K79 methylation patterns in meiotic mutants

To determine whether DOT1L and H3K79 methylation patterns are functionally tied to meiotic progression and/or recombination, we examined mutants affected at different stages during meiosis: *Spo11β*-only, $Trip13^{mod/mod}$, $Spo11^{-/-}$ and $Dmc1^{-/-}$ (Fig. 4, Supplementary Fig. 2, Supplementary Fig. 3 and Fig. 5, respectively; ordered from the one that reaches the furthest stage to the mutant with the least progression). These mutants exhibit defects in synapsis and/or recombination, with different degrees of severity that are incompatible with a successful meiosis program and lead to widespread checkpoint-induced arrest and apoptosis before the first meiotic division. The arrest point varies in the different male mouse mutants, but all are infertile (Barchi et al. 2005; Burgoyne et al. 2009; Handel and Schimenti 2010; Kauppi et al. 2011)

Spo11β-only—The $Spo11^{-/-}$ $Tg(Xmr\text{-}Spo11\beta B)^{+/+}$ transgenic mouse (hereafter, *Spo11β*-only) exclusively expresses the *Spo11β* splice variant, which is capable of supporting crossing-over, pairing, and synapsis normally in autosomes, but is defective in promoting late, efficient DSB formation specifically at the PAR (Kauppi et al. 2011). *Spo11β*-only spermatocytes frequently display X–Y association defects that trigger the spindle checkpoint causing apoptosis at metaphase I, so few spermatocytes reach later stages (Kauppi et al. 2011). We analyzed DOT1L localization and the H3K79me state in *Spo11β*-only from leptonema to diplonema (Fig. 4 and Supplementary Fig. 4a). Consistent with prior results, although some sperm were seen (note the sperm head in the lower left corner of the zygotene panel in Fig. 4a, asterisk), few spermatocytes at diakinesis or more advanced stages were found. Also as described previously, the X–Y chromosomes were unsynapsed in most sex bodies (surrounded in yellow in Fig. 4). *Spo11β*-only spermatocytes showed DOT1L staining similar to wild type: little or no signal at leptonema and zygonema, but significant signal during the pachytene and diplotene stages with accumulation at the sex body especially in diplotene nuclei (Fig. 4a and Supplementary Fig. 4a). H3K79me1 also showed no significant differences from control spermatocytes (Fig. 4b). In contrast, overall H3K79me2 levels were reduced in *Spo11β*-only diplotene nuclei relative to the wild type, although close to the control values for the remaining stages (Fig. 4c). As in the control, the H3K79me2 signal in the *Spo11β*-only sex body was lower than the average for the rest of the nucleus (Supplementary Fig. 4a). Finally, although H3K79me3 staining in *Spo11β*-only displayed the characteristic increasing trend throughout prophase I progression, the levels were significantly reduced during pachynema and diplonema (Fig. 4d). Nevertheless,

H3K79me3 was enriched at centromeric regions in the mutant (Fig. 4d and Supplementary Fig. 4b).

Trip13$^{mod/mod}$—We analyzed mice carrying a hypomorphic mutation of the yeast *PCH2* ortholog, *Trip13*, referred to as *Trip13$^{mod/mod}$* for "moderate" defect (Li et al. 2007; Roig et al. 2010). *Trip13$^{mod/mod}$* males show apparently fully synapsed chromosomes, but there is inefficient repair of meiotic DSBs, aberrant SC development and abnormal sex body formation, triggering a checkpoint response that leads to meiotic arrest and apoptosis at pachynema (Li et al. 2007; Wojtasz et al. 2009; Roig et al. 2010). We found no significant differences between wild type and *Trip13$^{mod/mod}$* spermatocytes with respect to either distribution or amount of DOT1L, H3K79me1, H3K79me2 or H3K79me3 in leptotene through pachytene spermatocytes (Supplementary Fig. 2a–d, respectively; too few spermatocytes at diplonema or further are found in this mutant, precluding analysis of later stages). H3K79me3 localization in the sex body and centromeric regions was also unaltered (Supplementary Fig. 2d and Supplementary Fig. 4c, d).

Spo11$^{-/-}$—This mutant lacks the evolutionary-conserved Spo11 transesterase that catalyzes meiotic DSBs, so it exhibits no meiotic recombination and fails in homolog pairing and synapsis. These defects trigger a DNA damage-independent checkpoint that leads to apoptosis at the zygotene-pachytene transition, a so-called zygotene-like stage (Baudat et al. 2000; Romanienko and Camerini-Otero 2000). We examined *Spo11$^{-/-}$* spermatocytes from leptotene to the zygotene-like stage, dividing the latter into two classes: early, with shorter SYCP3 stretches and low levels of axial association; and late, with full-length SYCP3 and extensive aberrant non-homologous synapsis (Supplementary Fig. 3). We found only very low levels of DOT1L and H3K79me1 staining throughout these stages in the *Spo11$^{-/-}$* mutant (Supplementary Fig. 3a, b). H3K79me2 and H3K79me3 increase slightly at the zygotene-like stage (Supplementary Fig. 3a, b), but in all cases, the signal intensity of DOT1L and all H3K79 methylation states was significantly reduced in the *Spo11$^{-/-}$* mutant (Supplementary Fig. 3).

Dmc1$^{-/-}$—The *Dmc1$^{-/-}$* mutant fails to repair meiotic DSBs and exhibits impaired synapsis, leading to arrest and apoptosis in a zygotene-like stage similar to that of *Spo11$^{-/-}$* (Pittman et al. 1998; Yoshida et al. 1998). However, molecular markers have revealed differences between the arrests in these two mutants. Specifically, unlike *Spo11$^{-/-}$*, *Dmc1$^{-/-}$* spermatocytes maintain the TopBP1 and γH2AX DNA damage checkpoint factors associated with chromatin, lack the H1t histone variant, and do not establish pseudo-sex bodies (Barchi et al. 2005). Therefore, although both mutants undergo apoptosis at a cytologically similar zygotene-like stage, molecular events indicate that *Dmc1$^{-/-}$* spermatocytes are arrested earlier. We monitored DOT1L and H3K79me in *Dmc1$^{-/-}$* from leptotene to zygotene-like stages (Fig. 5), divided into early and late categories, as above. Similar to *Spo11$^{-/-}$*, we found that the levels of DOT1L and all the H3K79 methylation states were significantly lower than in the wild-type control, especially in late zygotene-like spermatocytes (Fig. 5).

Sex body-specific dynamics of H3K79me3 and particular histone variants

To achieve MSCI, chromatin remodeling takes place in the sex body during pachynema. Histone H3 plays an important role in this process, via eviction of the canonical H3.1 and H3.2 forms and replacement by the H3.3 histone variant. As a consequence of this replacement, the PTMs carried by the H3.1/H3.2-H4 tetramers are removed; thus, the chance to establish new marks and/or the need to recover some of the lost ones emerges (van der Heijden et al. 2007). Other histone variants, such as H2A.Z, macroH2A and γH2AX, also exhibit remarkable changes during sex body development (Hoyer-Fender et al., 2000;

Fernandez-Capetillo et al., 2003; Greaves et al., 2006). Therefore, we compared the spatio-temporal pattern of DOT1L-dependent H3K79me3 at the sex body with that of those specific histone variants.

In agreement with previous observations (van der Heijden et al. 2007), we found an approximately four-fold enrichment for the H3.3 variant in the sex body during pachynema and diplonema (Fig. 6a, c). The incorporation of H3.3 appeared to be exclusive for the sex body, since the centromeric regions did not showed any particular accumulation of this histone variant (Fig. 6a). Total histone H3 distribution at these stages remained more uniform (Fig. 6b, c).

We found that the progressive enrichment of DOT1L in the sex body from early diplonema correlated with a decrease in γH2AX (Fig. 7a). In addition, the strong accumulation of H3K79me3 in the sex body during diakinesis-metaphase coincided with the complete disappearance of detectable γH2AX signal (Fig. 7b). Therefore, these two histone PTMs (H3K79me3 and γH2AX) are largely mutually exclusive, at least in the sex body. During these stages, H3K79me2 remained low and the H3K79me1 was uniformly weak (see above; Fig. 2b, c).

Finally, we analyzed the dynamics of the histone H2A variants macroH2A and H2A.Z in the sex body. The macroH2A variant defines heterochromatin areas, is enriched in the sex body from pachynema onward, participates in MSCI and disappears at later stages during diakinesis-metaphase I (Hoyer-Fender et al., 2000) (Supplementary Fig. 5a). In turn, it has been reported that the expression of H2A.Z begins in pachynema and peaks in round spermatids, supporting a role for H2A.Z in maintaining MSCI after disappearance of macroH2A and γH2AX (Greaves et al., 2006). We found H2A.Z all over the nucleus, except for strong exclusion from the sex body during pachynema and early-mid diplonema (Supplementary Fig. 5b, c). Then, H2A.Z became progressively more abundant in the sex body starting in late diplonema, reaching the same overall levels as the rest of the chromatin during diakinesis-metaphase I (Supplementary Fig. 5b, c). Therefore, whereas H3K79me3 exhibits limited coexistence with macroH2A at the sex body, its accumulation at this region correlates with the deposition of H2A.Z during late prophase I.

Discussion

In this paper we describe the localization of the histone methyltransferase DOT1L during male mouse meiotic prophase I. Since Dot1/DOT1L can mono-, di-, or tri-methylate H3K79, we also followed the dynamics of each individual methylation state resulting from DOT1L activity. Our cytological analyses show that the association of DOT1L with meiotic chromatin increases as prophase I progresses. Interestingly, although the H3K79me2 and H3K79me3 states, but not H3K79me1, also display a progressive increment, they show remarkable differences with respect to the subnuclear distribution, particularly in autosomal chromatin domains, centromeric chromatin, and the sex body. A summary of DOT1L localization and H3K79me patterns throughout prophase I is depicted in Fig. 8. The findings suggest that each H3K79 methylation state may have a specific role during mammalian spermatogenesis. This highly dynamic scenario contrasts with the situation in yeast, where global levels of H3K79me do not significantly change during meiosis (Ontoso et al. 2013). Although the precise chromosomal distribution of the different methylation states remains to be tested in yeast, it is likely that DOT1L activity during male mouse meiosis is subjected to a more complex regulation.

H3K79me3 in the sex body

Of the extensive chromatin remodeling that accompanies MSCI during early pachynema (Handel 2004; Turner 2007), one of the most dramatic changes is the replacement of histone H3.1/2 by the H3.3 variant, which implies the loss of most of the PTMs already established in the XY chromatin and the opportunity to introduce novel or additional marks (van der Heijden et al. 2007). Tri-methylation of histone H3 at other sites, such as H3K27, is among the repressive PTMs lost from the XY body during pachynema (van der Heijden et al. 2007). We find that the gradual increase of DOT1L all over the nucleus is especially evident in the sex body from diplonema onwards, coincident with the pronounced accumulation of H3.3. The H3.3 histone variant differs from H3.1 or H3.2 only in 5 or 4 amino acids, respectively (Supplementary Fig. 6a), and the H3K79 position, as well as the structure of nucleosomes containing either one of these three H3 variants, is conserved (Supplementary Fig. 6b–d) (Tachiwana et al. 2011). Moreover, in somatic mammalian cells, the presence of K79me1 and K79me2 in H3.3 has been reported (Hake et al. 2006; Sweet et al. 2010; Zee et al. 2010). Therefore, since DOT1L is the only methyltransferase known for H3K79, it is conceivable that DOT1L is responsible for the extensive tri-methylation of the H3.3 variant at K79 in the sex body during the late stages of meiotic prophase I (Fig. 1, 2). We note that there is a temporal shift between the prominent localization of DOT1L in the sex body (at diplonema) and the strong accumulation of H3K79me3 (at diakinesis). The additional regulation of DOT1L activity and/or substrate accessibility by other histone PTMs (i.e. H2BK120 ubiquitylation; McGinty et al. 2008) may account for this displacement.

H3K79me3 has been related with transcriptional repression in mammalian somatic cells (Barski et al. 2007). The H3K79me3 enrichment at the XY pair takes place during the diplotene/diakinesis transition when the staining for γH2AX and the repressive macroH2A variant becomes weaker. Nevertheless, it is possible that, although undetectable with our spreading technique, at least a fraction of these histone variants remains associated with the sex chromosomes until later meiotic stages, as occurs in other mammalian species (De la Fuente et al. 2007; Namekawa et al. 2007; De la Fuente et al. 2012). Conversely, H2A.Z, which is initially excluded from the sex body, arrives at this location at the same time as H3K79me3 accumulates. Most of the gene repression started with MSCI remains at postmeiotic stages, and may be linked with imprinted X-inactivation, although a subset of sex chromosome genes is upregulated postmeiotically (Namekawa et al. 2006; Mueller et al. 2008). As has been proposed for H2A.Z (Greaves et al. 2006) and other chromatin modifications, such as H3K9me2 and the recruitment of the heterochromatin proteins HP1β and HP1γ (Namekawa et al. 2006), our results are consistent with a role for DOT1L-mediated H3K79me3 in maintaining silencing of sex chromosomes from diplonema onwards. Curiously, in yeast, H2A.Z and H3K79 methylation also collaborate in the maintenance of differentiated chromatin domains contributing to the establishment of boundaries between the subtelomeric silenced chromatin and the active euchromatin (van Leeuwen et al., 2002; Ng et al., 2002; Meneghini et al., 2003). On the other hand, we demonstrate that the H3K79me2 mark, which is related with active transcription in somatic cells (Kouskouti and Talianidis 2005; Miao and Natarajan 2005; Zhou et al. 2011), remains largely excluded from the sex body with a faint signal only during late prophase I and metaphase I stages, presumably corresponding to the small fraction of X-linked genes expressed after MSCI (Mueller et al. 2008).

H3K79me3 at the centromeric heterochromatin

H3K79me3 also exhibits strong enrichment in the constitutive heterochromatin at centromeric regions during meiotic prophase I. This tendency was also reported in mouse somatic cells and oocytes, where H3K79me3 colocalizes with the heterochromatin protein HP1β (Ooga et al. 2008). Another histone PTM associated with transcriptional silencing,

such as H3K9me3 (Cowell et al. 2002; Wu et al. 2005), similarly accumulates at centromeric regions during mid-prophase I (Page et al. 2012). However, this mark has a wider localization all over the nucleus until mid-pachynema and, unlike H3K79me3, displays a reduced signal in the sex chromosomes from mid-pachynema onwards (Page et al. 2012), coincident with the replacement of H3.1/2 by H3.3. These observations are consistent with a specific role for H3K9me3 in transcriptional repression of the autosomes during early prophase I, and together with H3K79me3 in the establishment of centromeric heterochromatin. However, whereas the H3.3 newly incorporated at the sex body appears to be a favorable substrate for DOT1L and becomes highly tri-methylated at K79 during diplonema/diakinesis, it does not seem to be a target for the Suv39h methyltransferases responsible for H3K9me. Additional histone PTMs at centromeric regions, such as H3K9me2, H4K5ac and H4K16ac (ac, acetylation) also undergo particular dynamics during meiotic prophase I (Khalil and Driscoll 2010). Therefore, distinctive PTM combinations could set up spatial and temporal control of transcriptional repression or (re)activation during particular stages (Greaves et al. 2006; Namekawa et al. 2006; van der Heijden et al. 2007; Mueller et al. 2008; Khalil and Driscoll 2010; Page et al. 2012). Our results suggest that DOT1L-dependent H3K79me3 also impinges on this exquisite control. Consistent with a role for H3K79 methylation in heterochromatin formation it has been shown that DOT1L-deficient mouse embryonic stem cells possess reduced levels of constitutive heterochromatin marks, such as H4K20me3, at subtelomeric regions (Jones et al. 2008). Since DOT1L appears to be the only methyltransferase responsible for H3K79me in mouse (Jones et al. 2008), it is somehow surprising that the accumulation of H3K79me3 at centromeric domains does not correlate with stronger DOT1L staining in these regions. It is possible that the crosstalk with other(s) centromeric-specific histone PTMs may stimulate DOT1L activity specifically at these locations to reach higher levels of the maximum methylation state (i.e., H3K79me3). Alternatively, slower dynamics of histone H3 replacement at centromeres could also explain the accumulation of H3K79me3 (De Vos et al. 2011).

A potential role for H3K79me2 in autosomal transcriptional reactivation

In contrast to H3K79me3, we found a rather homogeneous distribution of H3K79me2 all over the nucleus, except for the exclusion from the sex body. Similar widespread localization has been described in mouse oocytes (Ooga et al. 2008). H3K79me2, like H3K4me3 and various H3 acetylation events, are characteristic marks of active genes in mammalian somatic cells (Kouskouti and Talianidis 2005; Miao and Natarajan 2005; Zhou et al. 2011). The H3K79me2 increase that we detect starting at pachynema and following DOT1L accumulation coincides temporally with the general transcriptional reactivation occurring on autosomes during the transition from mid to late pachynema and continuing in diplonema (Page et al. 2012). In addition, H3K79me2 distribution during prophase I exhibits a similar spatio-temporal pattern to that of H3K9ac and the active form of RNA polymerase II (RNAPII), both strongly associated with active transcription (Page et al. 2012). Furthermore, human DOT1L functionally interacts with actively transcribing RNAPII, which targets the methyltransferase to active genes (Kim et al. 2012a). Therefore, widespread DOT1L-dependent H3K79me2 from pachynema onwards could be an additional element contributing to the resumption of transcription in autosomes when recombination intermediates are resolved and characteristic marks, like γH2AX, and Dmc1/Rad51 foci, disappear. Alternatively, it could be also possible that accumulation of H3K79me2 is a consequence of transcriptional reactivation.

H3K79 methylation in challenged meiosis

Dot1/DOT1L-mediated H3K79me has multiple functions in a variety of biological processes from yeast to mammals (see Introduction; Nguyen and Zhang, 2011); but the functional contribution of Dot1 to meiosis has been investigated mostly in budding yeast. Dot1 is not

required in unperturbed meiosis, but is essential for the checkpoint responses to the accumulation of unrepaired meiotic DSBs and synapsis defects that occur in yeast *dmc1* and *zip1* mutants, respectively (San-Segundo and Roeder 2000; Ontoso et al. 2013). Unlike other chromatin marks, e.g. γH2AX, neither DOT1L nor H3K79me showed evidence for relocalization or redistribution in various mouse mutants defective at different steps in prophase I. The reduced levels of DOT1L, H3K79me2 and H3K79me3 at the latest stage of development reached in *Spo11*$^{-/-}$ and *Dmc1*$^{-/-}$ mutants are likely the consequence of the arrested meiosis that hampers the progressive accumulation of DOT1L observed in the wild type (Fig. 8). Higher levels of H3K79me2/3 are present in the *Spo11β*-only mouse, which shows milder meiotic defects, compared to the severely affected and prematurely arrested *Spo11*$^{-/-}$ and *Dmc1*$^{-/-}$ mutants, which barely accumulate those marks. The fact that DOT1L-dependent H3K79 modifications do not relocalize to sites of unrepaired DSBs or unsynapsed chromosomes in these mutants does not preclude a role for DOT1L in the mammalian checkpoints responding to meiotic defects. Actually, in the synapsis-defective *zip1* mutant of budding yeast, global H3K79me levels do not change compared with the wild type, despite the essential role of Dot1-dependent H3K79me in the checkpoint response promoting the *zip1* meiotic delay (Ontoso et al. 2013). Furthermore, in the DNA damage checkpoint triggered by unrepaired DSBs in somatic cells, a similar situation exists, because neither global nor local changes in H3K79 methylation occur, despite its role in the recruitment of mammalian 53BP1 or yeast Rad9 checkpoint adaptors (Huyen et al. 2004; Wysocki et al. 2005). Models involving chromatin remodeling events that locally expose methylated H3K79 residues under certain faulty circumstances have been invoked to explain these findings (Huyen et al. 2004; Wysocki et al. 2005; Ontoso et al. 2013). In the yeast *zip1* mutant, Dot1 promotes the accumulation of the HORMAD1/2 homolog Hop1 on unsynapsed axes to enable activation of the Mek1 checkpoint effector kinase. H3K79me-dependent chromosonal exclusion of the Trip13-homolog Pch2 contributes in part to the regulation of Hop1 localization (Ontoso et al. 2013). Although Pch2's checkpoint role is not restricted to yeast and it also exists in worms and flies (San-Segundo and Roeder 1999; Bhalla and Dernburg 2005; Joyce and McKim 2009), no evidence of the participation of Trip13 in mouse meiotic checkpoints has been found so far (Li et al. 2007; Roig et al. 2010). Therefore, if DOT1L also performs a meiotic checkpoint function in mouse it is unlikely to be exerted via Trip13 regulation.

Concluding remarks

Although functional interpretations from cytological analysis must be taken with caution, our results are consistent with a role for DOT1L and H3K79me at least in the special dynamics of chromatin repression/(re)activation that takes place during male mouse meiotic prophase I. Our observations open several intriguing questions, and more work needs to be done to expand our knowledge about DOT1L and H3K79me meiotic function(s) and regulation. For example, how is the same methyltransferase responsible for two methylated stages at the same target with such different roles? Undoubtedly, a fine regulation must be involved, perhaps mediated through the crosstalk with neighboring PTMs and/or histone variants in each moment and location. Alternatively, or in addition, the several DOT1L splicing isoforms in mice (Zhang et al. 2004) may have different affinities and/or requirements for catalytic activity, or the regulation could be imposed by other components of the DotCom complex (Mohan et al. 2010). Since DOT1L-knockout mice are not viable and die by embryonic day 10.5 (Jones et al., 2008), the development of conditional testis-specific DOT1L-deficient mice would be an invaluable tool to address the functional contribution of H3K79me to various meiotic events.

Supplementary Material

Refer to Web version on PubMed Central for supplementary material.

Acknowledgments

We thank the members of the SK and PSS laboratories for useful comments and discussion. We also thank the reviewers for their constructive comments and suggestions improving the manuscript. DO was supported by a predoctoral fellowship (JAE-Predoc) from the CSIC (Spain) and an EMBO short-term fellowship. Research was supported by NIH grant R01 GM105421 (to Maria Jasin and SK) and grants from MINECO (BFU2012-35748), Junta de Castilla y León (CSI025A11-2), and Fundación Ramón Areces to PSS.

References

Anglin JL, Deng L, Yao Y, Cai G, Liu Z, Jiang H, Cheng G, Chen P, et al. Synthesis and structure-activity relationship investigation of adenosine-containing inhibitors of histone methyltransferase DOT1L. J Med Chem. 2012; 55:8066–8074.10.1021/jm300917h [PubMed: 22924785]

Barchi M, Mahadevaiah S, Di Giacomo M, Baudat F, de Rooij DG, Burgoyne PS, Jasin M, Keeney S. Surveillance of different recombination defects in mouse spermatocytes yields distinct responses despite elimination at an identical developmental stage. Mol Cell Biol. 2005; 25:7203–7215.10.1128/MCB.25.16.7203-7215.2005 [PubMed: 16055729]

Barchi M, Roig I, Di Giacomo M, de Rooij DG, Keeney S, Jasin M. ATM promotes the obligate XY crossover and both crossover control and chromosome axis integrity on autosomes. PLoS Genet. 2008; 4:e1000076.10.1371/journal.pgen.1000076 [PubMed: 18497861]

Barry ER, Krueger W, Jakuba CM, Veilleux E, Ambrosi DJ, Nelson CE, Rasmussen TP. ES cell cycle progression and differentiation require the action of the histone methyltransferase Dot1L. Stem Cells. 2009; 27:1538–1547.10.1002/stem.86 [PubMed: 19544450]

Barski A, Cuddapah S, Cui K, Roh T-Y, Schones DE, Wang Z, Wei G, Chepelev I, et al. High-resolution profiling of histone methylations in the human genome. Cell. 2007; 129:823–837.10.1016/j.cell.2007.05.009 [PubMed: 17512414]

Baudat F, Manova K, Yuen JP, Jasin M, Keeney S. Chromosome synapsis defects and sexually dimorphic meiotic progression in mice lacking Spo11. Mol Cell. 2000; 6:989–998. [PubMed: 11106739]

Bernt KM, Zhu N, Sinha AU, Vempati S, Faber J, Krivtsov AV, Feng Z, Punt N, et al. MLL-rearranged leukemia is dependent on aberrant H3K79 methylation by DOT1L. Cancer Cell. 2011; 20:66–78.10.1016/j.ccr.2011.06.010 [PubMed: 21741597]

Bhalla N, Dernburg AF. A conserved checkpoint monitors meiotic chromosome synapsis in Caenorhabditis elegans. Science. 2005; 310:1683–1686.10.1126/science.1117468 [PubMed: 16339446]

Burgoyne PS, Mahadevaiah SK, Turner JMA. The consequences of asynapsis for mammalian meiosis. Nat Rev Genet. 2009; 10:207–216.10.1038/nrg2505 [PubMed: 19188923]

Castaño Betancourt MC, Cailotto F, Kerkhof HJ, Cornelis FMF, Doherty SA, Hart DJ, Hofman A, Luyten FP, et al. Genome-wide association and functional studies identify the DOT1L gene to be involved in cartilage thickness and hip osteoarthritis. Proc Natl Acad Sci U S A. 2012; 109:8218–8223.10.1073/pnas.1119899109 [PubMed: 22566624]

Cohen PE, Pollack SE, Pollard JW. Genetic analysis of chromosome pairing, recombination, and cell cycle control during first meiotic prophase in mammals. Endocr Rev. 2006; 27:398–426.10.1210/er.2005-0017 [PubMed: 16543383]

Cowell I, Aucott R, Mahadevaiah S, Huskisson N, Bongiorni S, Prantera G, Fanti L, Pimpinelli S, et al. Heterochromatin, HP1 and methylation at lysine 9 of histone H3 in animals. Chromosoma. 2002; 111:22–36.10.1007/s00412-002-0182-8 [PubMed: 12068920]

Daigle SR, Olhava EJ, Therkelsen CA, Majer CR, Sneeringer CJ, Song J, Johnston LD, Scott MP, et al. Selective killing of mixed lineage leukemia cells by a potent small-molecule DOT1L inhibitor. Cancer Cell. 2011; 20:53–65.10.1016/j.ccr.2011.06.009 [PubMed: 21741596]

de la Fuente R, Parra MT, Viera A, Calvente A, Gómez R, Suja JA, Rufas JS, Page J. Meiotic pairing and segregation of achiasmate sex chromosomes in eutherian mammals: the role of SYCP3 protein. PLoS Genet. 2007; 3:e198.10.1371/journal.pgen.0030198 [PubMed: 17983272]

de la Fuente R, Sánchez A, Marchal JA, Viera A, Parra MT, Rufas JS, Page J. A synaptonemal complex-derived mechanism for meiotic segregation precedes the evolutionary loss of homology between sex chromosomes in arvicolid mammals. Chromosoma. 2012; 121:433–446.10.1007/s00412-012-0374-9 [PubMed: 22552439]

De Vos D, Frederiks F, Terweij M, van Welsem T, Verzijlbergen KF, Iachina E, de Graaf EL, Maarten Altelaar AF, et al. Progressive methylation of ageing histones by Dot1 functions as a timer. EMBO Rep. 2011; 12:956–962.10.1038/embor.2011.131 [PubMed: 21760613]

Feng Q, Wang H, Ng HH, Erdjument-Bromage H, Tempst P, Struhl K, Zhang Y. Methylation of H3-lysine 79 is mediated by a new family of HMTases without a SET domain. Curr Biol. 2002; 12:1052–1058. [PubMed: 12123582]

Feng Y, Yang Y, Ortega MM, Copeland JN, Zhang M, Jacob JB, Fields TA, Vivian JL, et al. Early mammalian erythropoiesis requires the Dot1L methyltransferase. Blood. 2010; 116:4483–4491.10.1182/blood-2010-03-276501 [PubMed: 20798234]

Fernandez-Capetillo O, Mahadevaiah SK, Celeste A, Romanienko PJ, Camerini-Otero RD, Bonner WM, Manova K, Burgoyne P, et al. H2AX is required for chromatin remodeling and inactivation of sex chromosomes in male mouse meiosis. Dev Cell. 2003; 4:497–508. [PubMed: 12689589]

Frederiks F, Tzouros M, Oudgenoeg G, van Welsem T, Fornerod M, Krijgsveld J, van Leeuwen F. Nonprocessive methylation by Dot1 leads to functional redundancy of histone H3K79 methylation states. Nat Struct Mol Biol. 2008; 15:550–557.10.1038/nsmb.1432 [PubMed: 18511943]

Greaves IK, Rangasamy D, Devoy M, Marshall Graves JA, Tremethick DJ. The X and Y chromosomes assemble into H2A.Z, containing facultative heterochromatin, following meiosis. Mol Cell Biol. 2006; 26:5394–5405.10.1128/MCB.00519-06 [PubMed: 16809775]

Hake SB, Garcia BA, Duncan EM, Kauer M, Dellaire G, Shabanowitz J, Bazett- Jones DP, Allis CD, et al. Expression patterns and post-translational modifications associated with mammalian histone H3 variants. J Biol Chem. 2006; 281:559–568.10.1074/jbc.M509266200 [PubMed: 16267050]

Handel MA. The XY body: a specialized meiotic chromatin domain. Exp Cell Res. 2004; 296:57–63.10.1016/j.yexcr.2004.03.008 [PubMed: 15120994]

Handel MA, Schimenti JC. Genetics of mammalian meiosis: regulation, dynamics and impact on fertility. Nat Rev Genet. 2010; 11:124–136.10.1038/nrg2723 [PubMed: 20051984]

Hochwagen A, Amon A. Checking your breaks: surveillance mechanisms of meiotic recombination. Curr Biol. 2006; 16:R217–228.10.1016/j.cub.2006.03.009 [PubMed: 16546077]

Hoyer-Fender S, Costanzi C, Pehrson JR. Histone macroH2A1.2 is concentrated in the XY-body by the early pachytene stage of spermatogenesis. Exp Cell Res. 2000; 258:254–260.10.1006/excr.2000.4951 [PubMed: 10896776]

Huyen Y, Zgheib O, Ditullio RA, Gorgoulis VG, Zacharatos P, Petty TJ, Sheston EA, Mellert HS, et al. Methylated lysine 79 of histone H3 targets 53BP1 to DNA double-strand breaks. Nature. 2004; 432:406–411.10.1038/nature03114 [PubMed: 15525939]

Jo SY, Granowicz EM, Maillard I, Thomas D, Hess JL. Requirement for Dot1l in murine postnatal hematopoiesis and leukemogenesis by MLL translocation. Blood. 2011; 117:4759–4768.10.1182/blood-2010-12-327668 [PubMed: 21398221]

Jones B, Su H, Bhat A, Lei H, Bajko J, Hevi S, Baltus GA, Kadam S, et al. The histone H3K79 methyltransferase Dot1L is essential for mammalian development and heterochromatin structure. PLoS Genet. 2008; 4:e1000190.10.1371/journal.pgen.1000190 [PubMed: 18787701]

Joyce EF, McKim KS. Drosophila PCH2 is required for a pachytene checkpoint that monitors double-strand-break-independent events leading to meiotic crossover formation. Genetics. 2009; 181:39–51.10.1534/genetics.108.093112 [PubMed: 18957704]

Kauppi L, Barchi M, Baudat F, Romanienko PJ, Keeney S, Jasin M. Distinct properties of the XY pseudoautosomal region crucial for male meiosis. Science. 2011; 331:916–920.10.1126/science.1195774 [PubMed: 21330546]

Kalitsis P, Griffiths B, Choo KHA. Mouse telocentric sequences reveal a high rate of homogenization and possible role in Robertsonian translocation. Proc Natl Acad Sci U S A. 2006; 103:8786–8791.10.1073/pnas.0600250103 [PubMed: 16731628]

Keeney S. Spo11 and the formation of DNA double-strand breaks in meiosis. Genome Dyn Stab. 2008; 2:81–123.10.1007/7050_2007_026 [PubMed: 21927624]

Khalil AM, Driscoll DJ. Epigenetic regulation of pericentromeric heterochromatin during mammalian meiosis. Cytogenet Genome Res. 2010; 129:280–289.10.1159/000315903 [PubMed: 20606401]

Kim S-K, Jung I, Lee H, Kang K, Kim M, Jeong K, Kwon CS, Han Y-M, et al. Human histone H3K79 methyltransferase DOT1L binds actively transcribing RNA polymerase II to regulate gene expression. J Biol Chem. 2012a; 287:39698–39709.10.1074/jbc.M112.384057 [PubMed: 23012353]

Kim W, Kim R, Park G, Park J-W, Kim J-E. Deficiency of H3K79 histone methyltransferase Dot1-like protein (DOT1L) inhibits cell proliferation. J Biol Chem. 2012b; 287:5588–5599.10.1074/jbc.M111.328138 [PubMed: 22190683]

Kouskouti A, Talianidis I. Histone modifications defining active genes persist after transcriptional and mitotic inactivation. EMBO J. 2005; 24:347–357.10.1038/sj.emboj.7600516 [PubMed: 15616580]

Krivtsov AV, Feng Z, Lemieux ME, Faber J, Vempati S, Sinha AU, Xia X, Jesneck J, et al. H3K79 methylation profiles define murine and human MLL-AF4 leukemias. Cancer Cell. 2008; 14:355–368.10.1016/j.ccr.2008.10.001 [PubMed: 18977325]

Lacoste N, Utley RT, Hunter JM, Poirier GG, Côte J. Disruptor of telomeric silencing-1 is a chromatin-specific histone H3 methyltransferase. J Biol Chem. 2002; 277:30421–30424.10.1074/jbc.C200366200 [PubMed: 12097318]

Lammers JH, Offenberg HH, van Aalderen M, Vink AC, Dietrich AJ, Heyting C. The gene encoding a major component of the lateral elements of synaptonemal complexes of the rat is related to X-linked lymphocyte-regulated genes. Mol Cell Biol. 1994; 14:1137–1146.10.1128/MCB.14.2.1137.Updated [PubMed: 8289794]

Li XC, Li X, Schimenti JC. Mouse Pachytene Checkpoint 2 (Trip13) is required for completing meiotic recombination but not synapsis. PLoS Genet. 2007; 3:e130.10.1371/journal.pgen.0030130 [PubMed: 17696610]

Liebe B, Alsheimer M, Höög C, Benavente R, Scherthan H. Telomere attachment, meiotic chromosome condensation, pairing, and bouquet stage duration are modified in spermatocytes lacking axial elements. Mol Biol Cell. 2004; 15:827–837.10.1091/mbc.E03-07-0524 [PubMed: 14657244]

Macqueen AJ, Hochwagen A. Checkpoint mechanisms: the puppet masters of meiotic prophase. Trends Cell Biol. 2011; 21:393–400.10.1016/j.tcb.2011.03.004 [PubMed: 21531561]

McGinty RK, Kim J, Chatterjee C, Roeder RG, Muir TW. Chemically ubiquitylated histone H2B stimulates hDot1L-mediated intranucleosomal methylation. Nature. 2008; 453:812–816.10.1038/nature06906 [PubMed: 18449190]

Meneghini MD, Wu M, Madhani HD. Conserved histone variant H2A.Z protects euchromatin from the ectopic spread of silent heterochromatin. Cell. 2003; 112:725–736. [PubMed: 12628191]

Miao F, Natarajan R. Mapping global histone methylation patterns in the coding regions of human genes. Mol Cell Biol. 2005; 25:4650–4661.10.1128/MCB.25.11.4650-4661.2005 [PubMed: 15899867]

Mohan M, Herz H, Takahashi Y, Lin C, Lai KC, Zhang Y, Washburn MP, Florens L, et al. Linking H3K79 trimethylation to Wnt signaling through a novel Dot1-containing complex (DotCom). Genes Dev. 2010; 24:574–589.10.1101/gad.1898410 [PubMed: 20203130]

Mueller JL, Mahadevaiah SK, Park PJ, Warburton PE, Page DC, Turner JMA. The mouse X chromosome is enriched for multicopy testis genes showing postmeiotic expression. Nat Genet. 2008; 40:794–799.10.1038/ng.126 [PubMed: 18454149]

Namekawa SH, Park PJ, Zhang L-F, Shima JE, McCarrey JR, Griswold MD, Lee JT. Postmeiotic sex chromatin in the male germline of mice. Curr Biol. 2006; 16:660–667.10.1016/j.cub.2006.01.066 [PubMed: 16581510]

Namekawa SH, VandeBerg JL, McCarrey JR, Lee JT. Sex chromosome silencing in the marsupial male germ line. Proc Natl Acad Sci U S A. 2007; 104:9730–9735.10.1073/pnas.0700323104 [PubMed: 17535928]

Ng HH, Feng Q, Wang H, Erdjument-Bromage H, Tempst P, Zhang Y, Struhl K. Lysine methylation within the globular domain of histone H3 by Dot1 is important for telomeric silencing and Sir protein association. Genes Dev. 2002; 16:1518–1527.10.1101/gad.1001502 [PubMed: 12080090]

Ng HH, Ciccone DN, Morshead KB, Oettinger MA, Struhl K. Lysine-79 of histone H3 is hypomethylated at silenced loci in yeast and mammalian cells: a potential mechanism for position-effect variegation. Proc Natl Acad Sci U S A. 2003; 100:1820–1825.10.1073/pnas.0437846100 [PubMed: 12574507]

Nguyen AT, Xiao B, Neppl RL, Kallin EM, Li J, Chen T, Wang D-Z, Xiao X, et al. DOT1L regulates dystrophin expression and is critical for cardiac function. Genes Dev. 2011; 25:263–274.10.1101/gad.2018511 [PubMed: 21289070]

Nguyen AT, Zhang Y. The diverse functions of Dot1 and H3K79 methylation. Genes Dev. 2011; 25:1345–1358.10.1101/gad.2057811 [PubMed: 21724828]

Okada Y, Feng Q, Lin Y, Jiang Q, Li Y, Coffield VM, Su L, Xu G, et al. hDOT1L links histone methylation to leukemogenesis. Cell. 2005; 121:167–178.10.1016/j.cell.2005.02.020 [PubMed: 15851025]

Ontoso D, Acosta I, van Leeuwen F, Freire R, San-Segundo PA. Dot1-dependent histone H3K79 methylation promotes activation of the Mek1 meiotic checkpoint effector kinase by regulating the Hop1 adaptor. PLoS Genet. 2013; 9:e1003262.10.1371/journal.pgen.1003262 [PubMed: 23382701]

Ooga M, Inoue A, Kageyama S, Akiyama T, Nagata M, Aoki F. Changes in H3K79 methylation during preimplantation development in mice. Biol Reprod. 2008; 78:413–424.10.1095/biolreprod.107.063453 [PubMed: 18003948]

Page J, de la Fuente R, Manterola M, Parra MT, Viera A, Berríos S, Fernández-Donoso R, Rufas JS. Inactivation or non-reactivation: what accounts better for the silence of sex chromosomes during mammalian male meiosis? Chromosoma. 2012; 121:307–326.10.1007/s00412-012-0364-y [PubMed: 22366883]

Parra MT, Viera A, Gómez R, Page J, Benavente R, Santos JL, Rufas JS, Suja JA. Involvement of the cohesin Rad21 and SCP3 in monopolar attachment of sister kinetochores during mouse meiosis I. J Cell Sci. 2004; 117:1221–1234.10.1242/jcs.00947 [PubMed: 14970259]

Pawlowski WP, Cande WZ. Coordinating the events of the meiotic prophase. Trends Cell Biol. 2005; 15:674–681.10.1016/j.tcb.2005.10.005 [PubMed: 16257210]

Pittman DL, Cobb J, Schimenti KJ, Wilson LA, Cooper DM, Brignull E, Handel MA, Schimenti JC. Meiotic prophase arrest with failure of chromosome synapsis in mice deficient for Dmc1, a germline-specific RecA homolog. Mol Cell. 1998; 1:697–705. [PubMed: 9660953]

Roig I, Dowdle JA, Toth A, de Rooij DG, Jasin M, Keeney S. Mouse TRIP13/PCH2 is required for recombination and normal higher-order chromosome structure during meiosis. PLoS Genet. 2010; 6:e1001062.10.1371/journal.pgen.1001062 [PubMed: 20711356]

Romanienko PJ, Camerini-Otero RD. The mouse Spo11 gene is required for meiotic chromosome synapsis. Mol Cell. 2000; 6:975–987. [PubMed: 11106738]

San-Segundo PA, Roeder GS. Pch2 links chromatin silencing to meiotic checkpoint control. Cell. 1999; 97:313–324. [PubMed: 10319812]

San-Segundo PA, Roeder GS. Role for the silencing protein Dot1 in meiotic checkpoint control. Mol Biol Cell. 2000; 11:3601–3615. [PubMed: 11029058]

Steger DJ, Lefterova MI, Ying L, Stonestrom AJ, Schupp M, Zhuo D, Vakoc AL, Kim J-E, et al. DOT1L/KMT4 recruitment and H3K79 methylation are ubiquitously coupled with gene transcription in mammalian cells. Mol Cell Biol. 2008; 28:2825–2839.10.1128/MCB.02076-07 [PubMed: 18285465]

Sweet SMM, Li M, Thomas PM, Durbin KR, Kelleher NL. Kinetics of reestablishing H3K79 methylation marks in global human chromatin. J Biol Chem. 2010; 285:32778–32786.10.1074/jbc.M110.145094 [PubMed: 20699226]

Tachiwana H, Kagawa W, Osakabe A, Kawaguchi K, Shiga T, Hayashi-Takanaka Y, Kimura H, Kurumizaka H. Structural basis of instability of the nucleosome containing a testis-specific histone variant, human H3T. Proc Natl Acad Sci U S A. 2010; 107:10454–10459.10.1073/pnas.1003064107 [PubMed: 20498094]

Tachiwana H, Osakabe A, Shiga T, Miya Y, Kimura H, Kagawa W, Kurumizaka H. Structures of human nucleosomes containing major histone H3 variants. Acta Crystallogr D Biol Crystallogr. 2011; 67:578–583.10.1107/S0907444911014818 [PubMed: 21636898]

Turner JMA. Meiotic sex chromosome inactivation. Development. 2007; 134:1823–1831.10.1242/dev.000018 [PubMed: 17329371]

van der Heijden GW, Derijck AAHA, Pósfai E, Giele M, Pelczar P, Ramos L, Wansink DG, van der Vlag J, et al. Chromosome-wide nucleosome replacement and H3.3 incorporation during mammalian meiotic sex chromosome inactivation. Nat Genet. 2007; 39:251–258.10.1038/ng1949 [PubMed: 17237782]

van Leeuwen F, Gafken PR, Gottschling DE. Dot1p modulates silencing in yeast by methylation of the nucleosome core. Cell. 2002; 109:745–756. [PubMed: 12086673]

Wojtasz L, Daniel K, Roig I, Bolcun-Filas E, Xu H, Boonsanay V, Eckmann CR, Cooke HJ, et al. Mouse HORMAD1 and HORMAD2, two conserved meiotic chromosomal proteins, are depleted from synapsed chromosome axes with the help of TRIP13 AAA-ATPase. PLoS Genet. 2009; 5:e1000702.10.1371/journal.pgen.1000702 [PubMed: 19851446]

Wu R, Terry AV, Singh PB, Gilbert DM. Differential subnuclear localization and replication timing of histone H3 lysine 9 methylation states. Mol Biol Cell. 2005; 16:2872–2881.10.1091/mbc.E04 [PubMed: 15788566]

Wysocki R, Javaheri A, Allard S, Sha F, Côté J, Kron SJ. Role of Dot1-dependent histone H3 methylation in G1 and S phase DNA damage checkpoint functions of Rad9. Mol Cell Biol. 2005; 25:8430–8443.10.1128/MCB.25.19.8430-8443.2005 [PubMed: 16166626]

Yao Y, Chen P, Diao J, Cheng G, Deng L, Anglin JL, Prasad BVV, Song Y. Selective inhibitors of histone methyltransferase DOT1L: design, synthesis, and crystallographic studies. J Am Chem Soc. 2011; 133:16746–16749.10.1021/ja206312b [PubMed: 21936531]

Yoshida K, Kondoh G, Matsuda Y, Habu T, Nishimune Y, Morita T. The mouse RecA-like gene Dmc1 is required for homologous chromosome synapsis during meiosis. Mol Cell. 1998; 1:707–718. [PubMed: 9660954]

Zee BM, Levin RS, Dimaggio PA, Garcia BA. Global turnover of histone post-translational modifications and variants in human cells. Epigenetics & Chromatin. 2010; 3:22.10.1186/1756-8935-3-22 [PubMed: 21134274]

Zhang Q, Xue P, Li H, Bao Y, Wu L, Chang S, Niu B, Yang F, et al. Histone modification mapping in human brain reveals aberrant expression of histone H3 lysine 79 dimethylation in neural tube defects. Neurobiol Dis. 2013; 54:404–413.10.1016/j.nbd.2013.01.014 [PubMed: 23376398]

Zhang W, Hayashizaki Y, Kone BC. Structure and regulation of the mDot1 gene, a mouse histone H3 methyltransferase. Biochem J. 2004; 377:641–651.10.1042/BJ20030839 [PubMed: 14572310]

Zhou VW, Goren A, Bernstein BE. Charting histone modifications and the functional organization of mammalian genomes. Nat Rev Genet. 2011; 12:7–18.10.1038/nrg2905 [PubMed: 21116306]

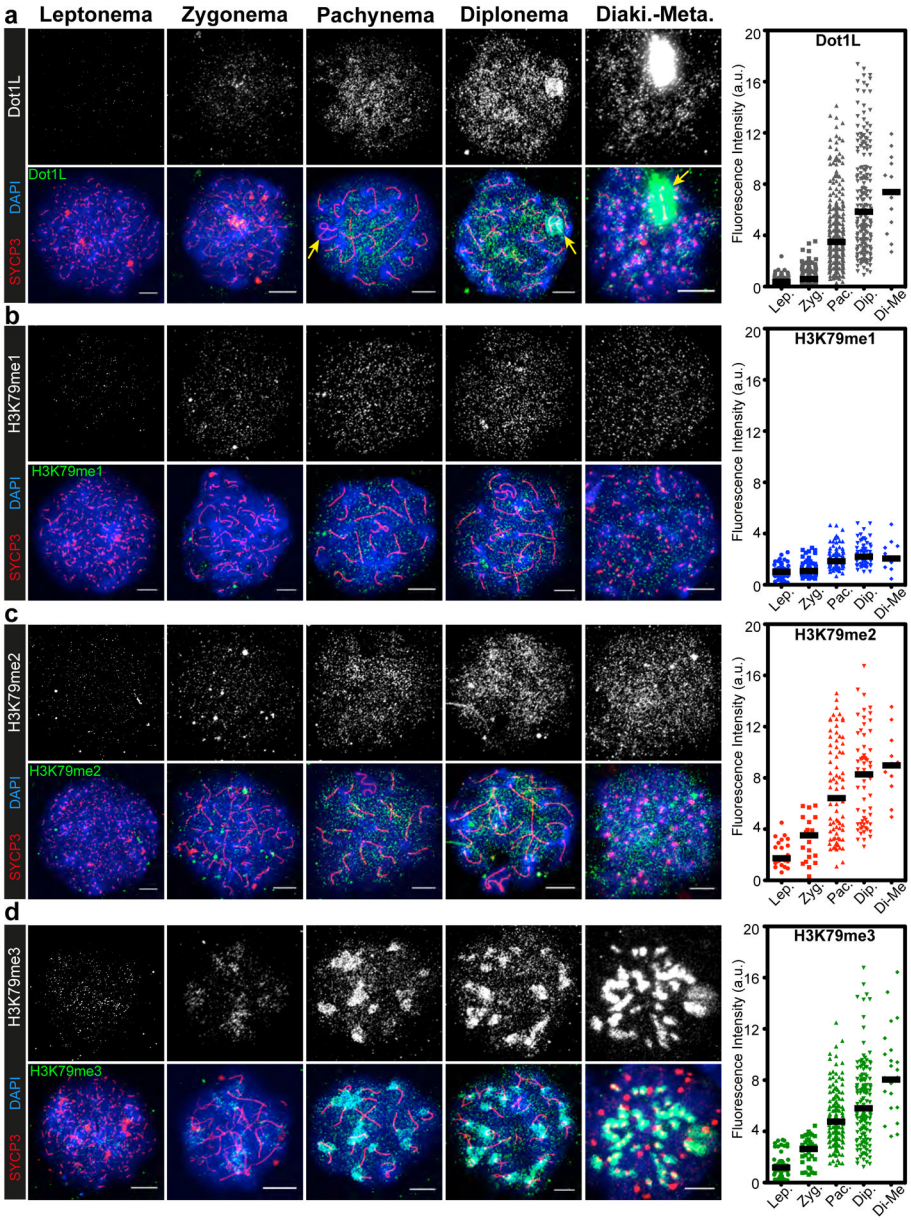

Fig. 1.

DOT1L and H3K79me localization patterns throughout male mouse meiotic prophase I. **a–d** Immunofluorescence of surface-spread wild-type spermatocytes stained with antibodies to SYCP3 (red) and to either DOT1L (**a**), H3K79me1 (**b**), H3K79me2 (**c**) or H3K79me3 (**d**), shown in white or green, as indicated on the panels. DAPI staining of chromatin is shown in blue. Representative nuclei for each prophase I stage are presented, determined by the SYCP3 localization pattern (see also Supplementary Fig. 1). In **a**, the sex body is pointed by a yellow arrow. Quantification of the signal intensity for DOT1L and the different H3K79me states is shown in arbitrary units (a.u.) on the right graphs. Each dot in the scatter plot indicates the value for an individual nucleus. The central horizontal line is the median. Scale bar: 10 μm.

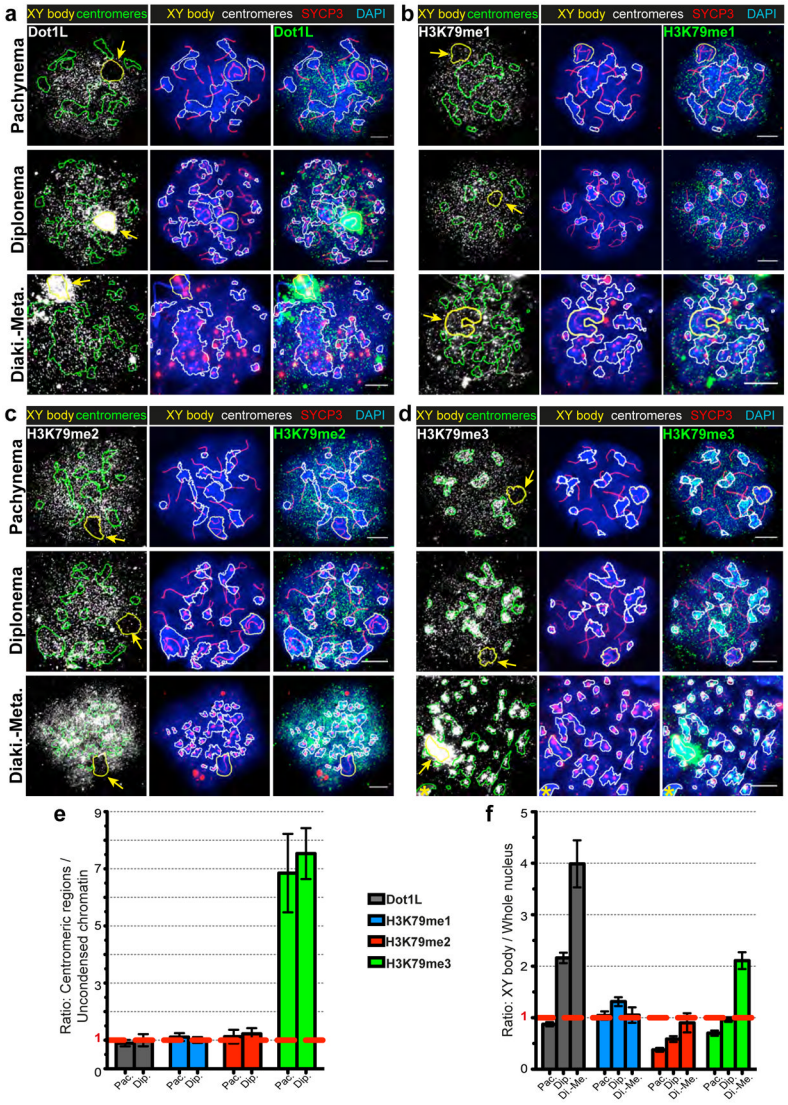

Fig. 2.

Subnuclear distribution of DOT1L and H3K79me. **a–d** Localization of DOT1L (**a**), H3K79me1 (**b**), H3K79me2 (**c**) and H3K79me3 (**d**) in representative pachytene, diplotene and diakinesis-metaphase nuclei. In every group of panels, the left column is for either DOT1L or each particular H3K79me state (white), with the centromeric areas (centromeres) outlined in green, and the sex body outlined in yellow and marked with an arrow. The central column is the merge of SYCP3 (red) and DAPI (blue), with the centromeric areas (centromeres) outlined in white and the sex body in yellow. The right column additionally displays DOT1L or the corresponding H3K79me state in green. Yellow asterisks mark adjacent cells. Scale bar: 10 μm. **e** Ratio of the area of centromeric regions containing DOT1L or H3K79me signal, relative to the area of the remaining uncondensed autosomal chromatin domains with the corresponding signal. **f** Ratio of the area of the sex body with DOT1L or H3K79me signal, relative to the area of the whole nucleus with signal (excluding the sex body). A more detailed explanation of quantification could be found in the Materials and methods section. Pac, pachynema; Dip, diplonema and Di.-Me., diakinesis-metaphase I. Error bars are the standard error of mean (SEM).

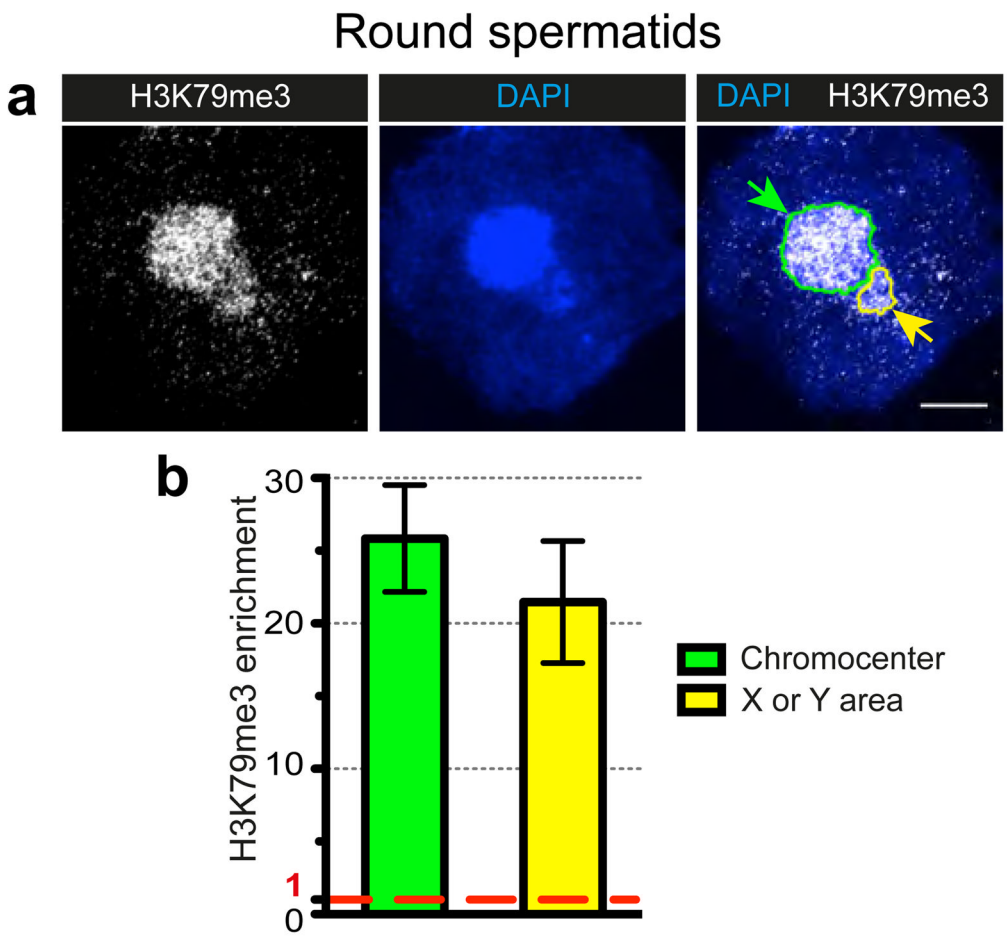

Fig. 3.

H3K79me3 accumulates in the chromocenter and the sex chromosome domain at post-meiotic stages. **a** A representative round spermatid stained with DAPI (blue) and antibodies to H3K79me3 (white) is shown. The chromocenter (green arrow) and the sex chromosome, X or Y, domain (yellow arrow), displaying differential DAPI intensities, are outlined on the merged panel. **b** Quantification of the H3K79me3 signal present in the chromocenter (green bar) and the sex chromosome (yellow bar) relative to the signal in the remaining uncondensed chromatin. 15 spermatids were quantified. Scale bar: 10 μm.

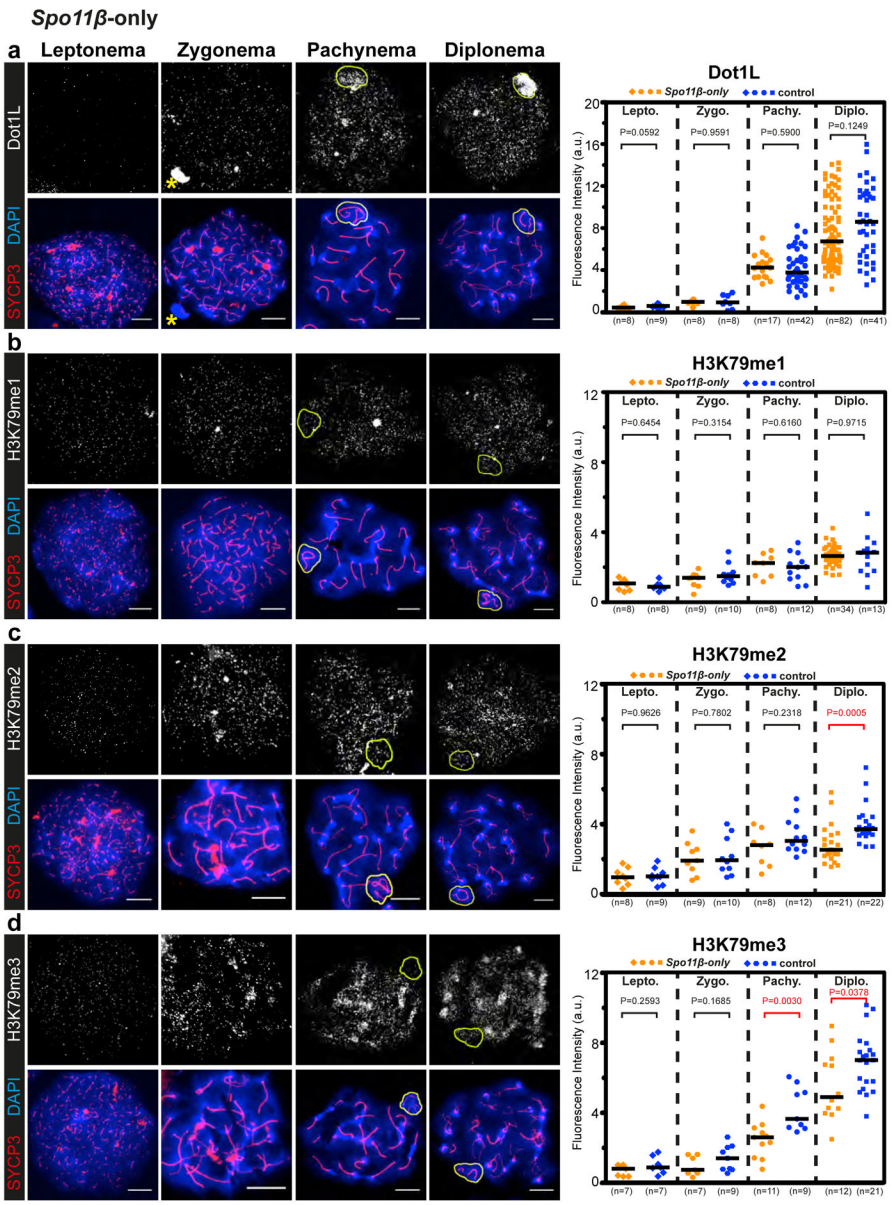

Fig. 4.

DOT1L and H3K79 methylation patterns in the *Spo11β*-only mutant. **a–d** Immunofluorescence of surface-spread spermatocytes from the *Spo11β*-only mutant stained with antibodies to SYCP3 (red) and either DOT1L (**a**), H3K79me1 (**b**), H3K79me2 (**c**) or H3K79me3 (**d**) shown in white. DAPI staining of chromatin is shown in blue. Representative nuclei for the indicated prophase I stages are presented. The sex body is outlined in yellow. Scale bar, 10 μm. The scatter plots show the quantification of the indicated immunofluorescence signal (a.u., arbitrary units) in spermatocytes from the *Spo11β*-only mutant and a littermate heterozygous control [$Spo11^{+/-}$ $Tg(Xmr\text{-}Spo11\beta B)^{+/+}$]. Each dot in the graph indicates the value for an individual nucleus. The central horizontal line is the median and “n” is the number of nuclei evaluated at each stage. *P*-values were calculated by two-tailed Mann-Whitney tests of the indicated pairwise comparisons. $P<0.05$ was considered statistically significant (marked in red).

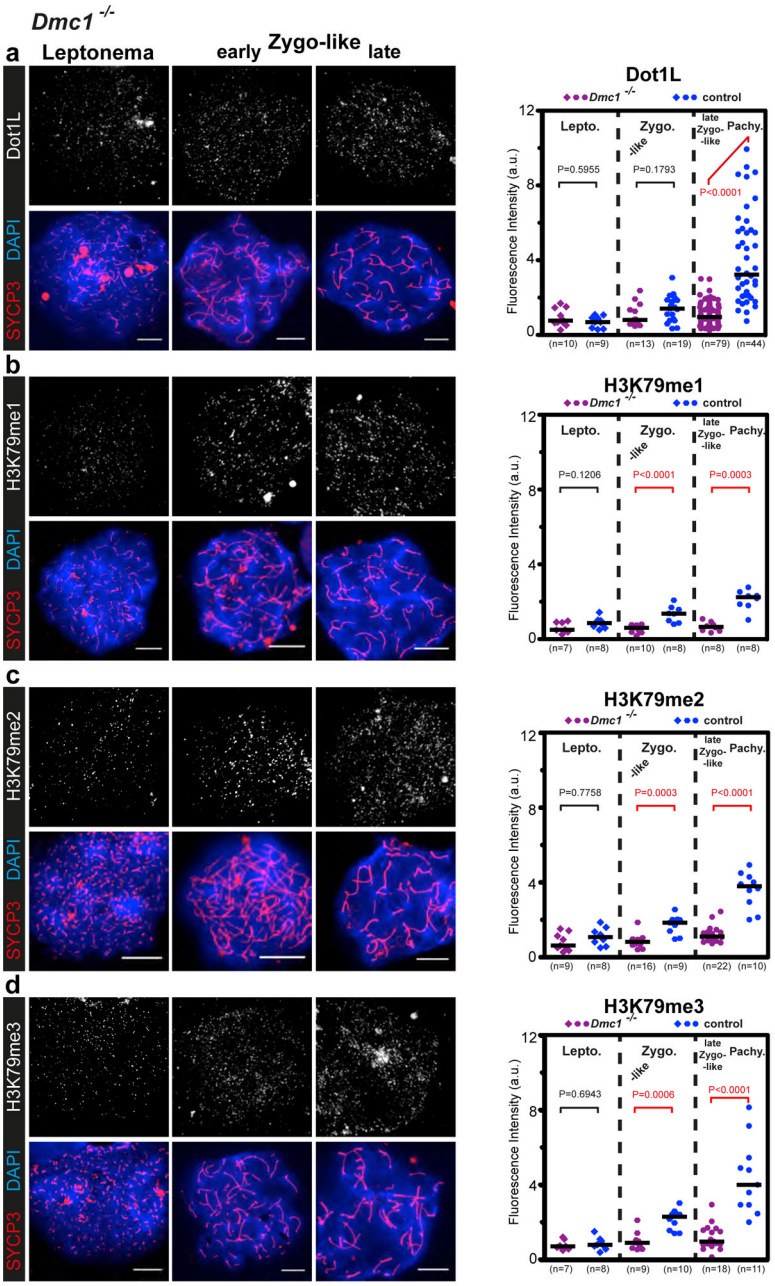

Fig. 5.

DOT1L and H3K79 methylation patterns in the *Dmc1*$^{-/-}$ mutant. **a–d** Spermatocytes from the *Dmc1*$^{-/-}$ mutant and a littermate *Dmc1*$^{+/-}$ control were analyzed as indicated in Fig. 4.

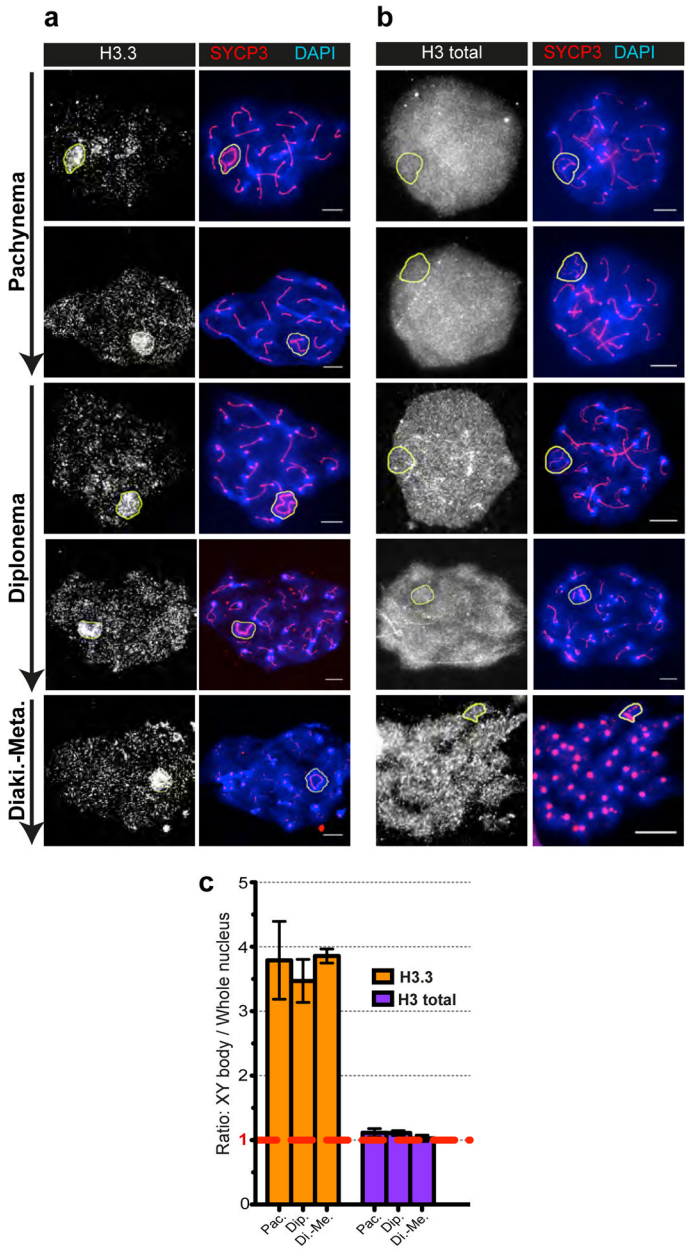

Fig. 6.

Enrichment of the H3.3 histone variant in the sex body. **a, b** Immunofluorescence of surface-spread wild-type spermatocytes stained with antibodies specific to the H3.3 histone variant (**a**; white color) and total histone H3 (**b**; white color). The merged images of SYCP3 (red) and DAPI (blue) are also shown. Representative nuclei for the indicated prophase I stages, determined by the SYCP3 localization pattern, are presented. The sex body is outlined in yellow. Scale bars: 10 μm. **c** Ratio of the area of the sex body with H3.3 (orange bars) or total H3 (purple bars) signal, relative to the area of the whole nucleus with signal (excluding the sex body). Pac, pachynema; Dip, diplonema and Di.-Me., diakinesis-metaphase. Error bars are the standard error of mean (SEM).

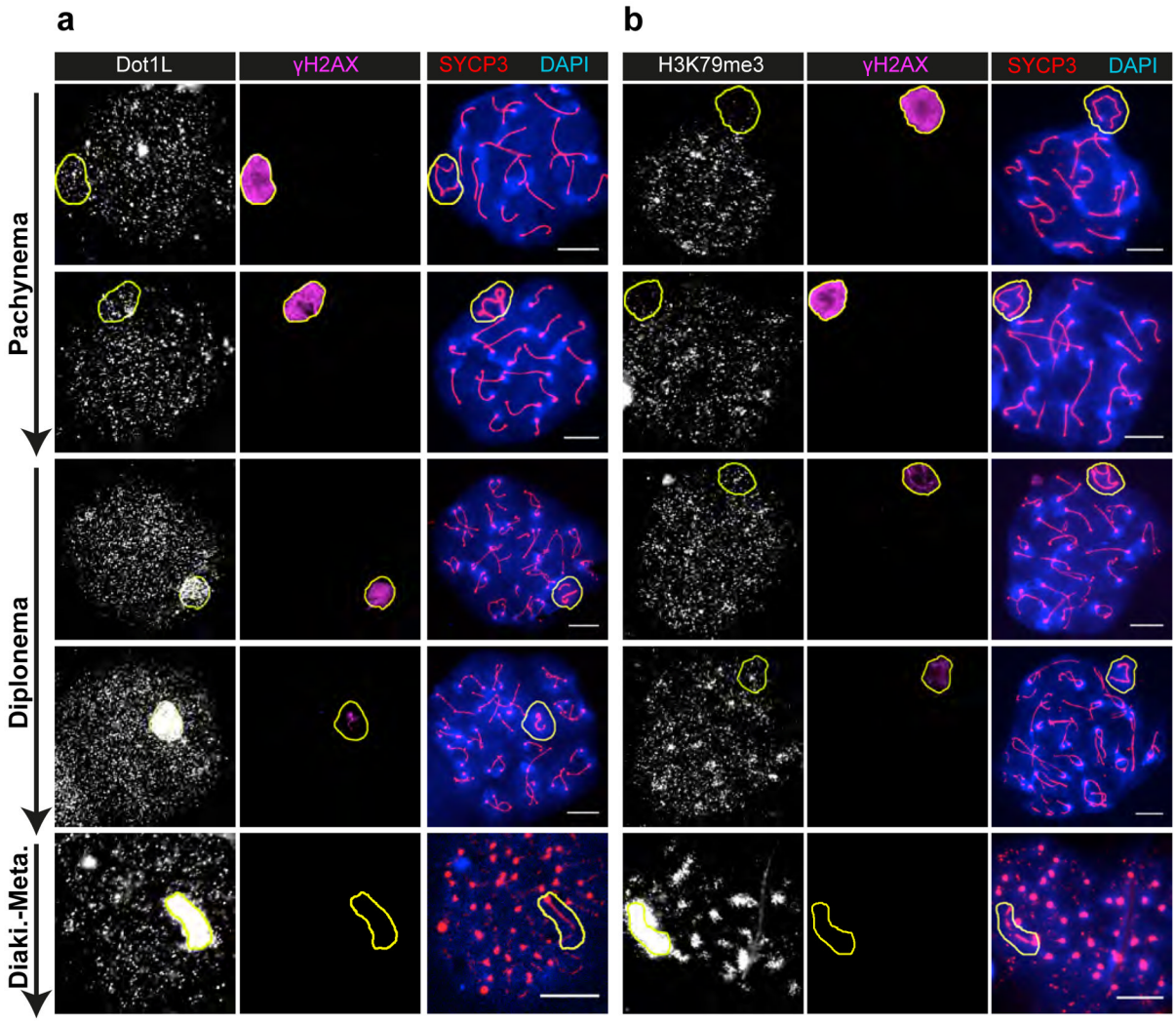

Fig. 7.

Accumulation of γH2AX and DOT1L/H3K79me3 at the sex body display largely opposite dynamics. Representative nuclei for pachytene, diplotene and diakinesis-metaphase I stages stained with antibodies to DOT1L (white) and γH2AX (purple) in (**a**), or antibodies to H3K79me3 (white) and γH2AX (purple) in (**b**). The merged images of SYCP3 (red) and DAPI (blue) are also shown. The XY body is outlined in yellow. Scale bars: 10 μm.

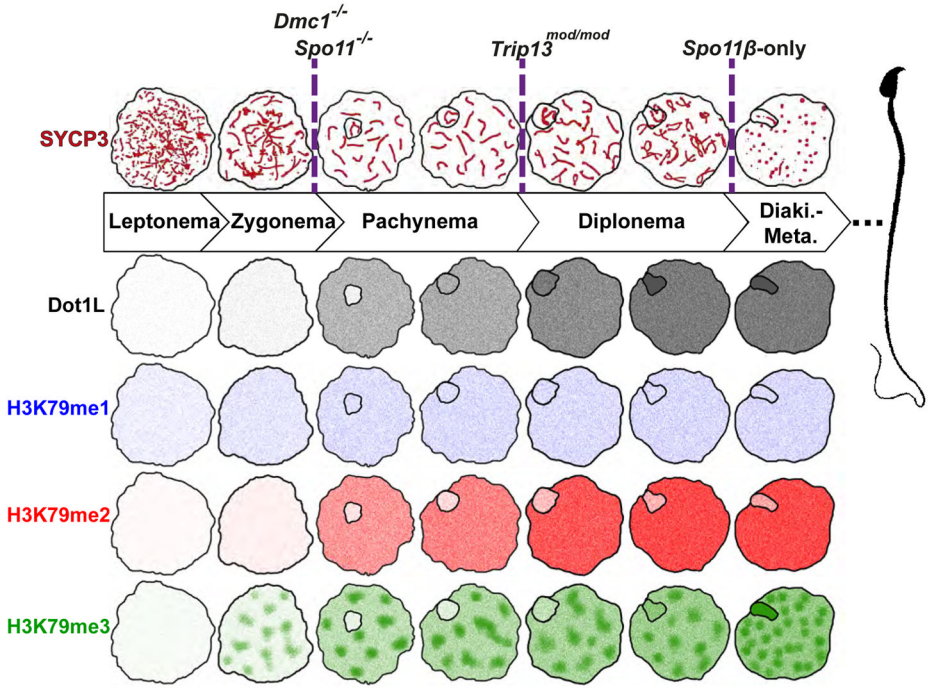

Fig. 8.

Summary of DOT1L and H3K79me localization patterns throughout prophase I in mouse spermatocytes. Schematic representation of spermatocytes at different stages of prophase I displaying the characteristic arrangement of SYCP3 (dark red lines) and the corresponding pattern for DOT1L (grey), H3K79me1 (blue), H3K79me2 (red) and H3K79me3 (green). The color gradation reflects the signal intensity for each marker. The sex body is outlined. The dashed purple lines mark the last developmental stage reached by each mutant analyzed (see text for details).